

Opportunities and Dilemmas of *In Vitro* Nano Neural Electrodes

Yu Wu,^a Haowen Chen^a and Liang Guo^{*a}

Received 00th January 20xx,
Accepted 00th January 20xx

DOI: 10.1039/x0xx00000x

Abstract: Developing electrophysiological platforms to capture electrical activities of neurons and exert modulatory stimuli lays the foundation for many neuroscience-related disciplines, including neuron-machine interface, neuroprosthesis, and mapping of brain circuitry. Intrinsically more advantageous than genetic and chemical neuronal probes, electrical interfaces directly target the fundamental driving force — transmembrane currents — behind the complicated and diverse neuronal signals, allowing for discovering neural computation mechanisms at the most accurate extent. Furthermore, establishing electrical access to neurons is so far the most promising solution to integrate the large-scale, high-speed modern electronics with neurons that are highly dynamic and adaptive. Over the evolution of electrode-based electrophysiologies, it has long been a trade-off among precision, invasiveness, and parallel access due to limitations on fabrication techniques and insufficient understanding of membrane-electrode interactions. On the one hand, intracellular platforms based on patch clamps and sharp electrodes suffer from the acute cellular damage, fluid diffusion, and labor-intensive micromanipulation with little room for parallel recordings. On the other hand, conventional extracellular microelectrode arrays cannot detect from subcellular compartments or capture subthreshold membrane potentials because of the large electrode size and poor seal resistance, making it impossible to depict a comprehensive picture of a neuron's electrical activities. Recently, the application of nanotechnology on neuronal electrophysiology has brought a promising solution to mitigate these conflicts on a single chip. Particularly, three dimensional nanostructures of 10 – 100 nm diameter are naturally fit to achieve the purpose of precise and localized interrogations. And engineering them into vertical nanoprobe bound on planar substrates resulted in excellent membrane-electrode seals and high-density electrode distribution. It is no doubt that 3D vertical nanoelectrodes have achieved a fundamental milestone of high precision, low invasiveness, and parallel recording at neuron-electrode interface, albeit with substantial engineering issues to fully exploit the potential of nano neural interfaces. Within this framework, we review the qualitative breakthroughs and opportunities brought by 3D vertical nanoelectrodes, and discuss on the major limitations of current electrode designs with respect to rational and seamless cell-on-chip systems.

Introduction

Electrogenic neurons, as the control units of most biological livings, have great potentials in advancing life technologies and artificial intelligences. In the central nervous system, neuronal networks are able to learn adaptively from environmental inputs, form cognitions, and carry memory storage. In the peripheral nervous system, neurons can sense a diversity of mechanical, chemical, and thermal stimuli, while delivering accurate controls through neuromuscular junctions for both long-range, high-strength and short-range, delicate motions. Moreover, the highly efficient transformation from chemical energy to ionic gradients allows a neuron to generate and transmit electric signals. Therefore, it has long been a major pursuit in neuroscience, bioengineering, and electrical engineering to develop seamless neural interfaces for probing, understanding, and modulating neural activities. And despite advances in engineering large-scale electrophysiological approaches for *in vivo* applications [1-7], establishing neuronal

interfaces at the cellular and subcellular levels *in vitro* is still imperative to answer the fundamental questions of how to achieve high-fidelity and reliable cell-to-chip communications.

At the implementation level, constructing a bridge between electronic devices and neurons requires the electrodes not only to have appropriate electrical properties for signal detection and/or current injection, but also to be able to adapt to the dynamic and fragile nature of cells. Conventional tools of intracellular micropipettes (e.g. patch clamps) and extracellular microelectrode arrays (MEAs) have intrinsically suffered from the trade-off between invasiveness and precision. Patch clamp often lead to severe cell damage within hours from electrode insertion, and are difficult to expand to multisite, parallel recordings. While the planar MEAs impose no invasiveness to cells, the large dimension of electrode size (often close to or bigger than neuronal soma) and poor electrode-membrane seal make it difficult to reveal subcellular and subthreshold neuronal activities. Looking back at nature, the nanoscale ion channels are the driving forces behind the great diversity of neuronal dynamics, which provides a biomimetic inspiration to overcome this trade-off by shrinking the electrode dimensions to the nanoscale. Although a variety of nanostructures, such as planar nanowires and suspended nanoparticles [8-13], were applied to neuronal recording and stimulation, the revolutionary

^a Department of Electrical and Computer Engineering, The Ohio State University, Columbus, OH, USA.

*Email: guo.725@osu.edu.

breakthrough towards organized and high-resolution neural interface was enabled by the 3D nanofabrication techniques. Vertical nanoelectrode arrays significantly reduced the projection area on the planar substrate they bound without compromising the interfacial area with local cell membrane, allowing for the realization of high-density fabrication and parallel recording from different compartments of single neurons. More importantly, their topography of 3D protrusions provides intimate electrode-membrane seals, drastically improving the reliability and fidelity of recording. In this way, nanoelectrode arrays not only induce sufficient invasiveness to ensure high-quality signals, but also cause minimal cellular damages even after electrical or optical porations. Therefore, these advantages from scaling down to the nanoscale have provided new possibilities for solid-state electronics to “talk” with electrogenic neurons.

In this focused review, we will discuss the fundamental advantages and issues of *in vitro* nano neural electrodes towards the goal of accurate and rational cell-machine interfaces, primarily focusing on vertical nanoelectrode arrays that are most promising for large-scale, parallel neuronal interfaces. Specifically, we start with the neuronal computation process enabled by nanoscale ion channels and neuronal projections, as well as a brief overview on the electrical interface between nanoelectrodes and neurons. Next, we highlight the opportunities provided by nanoelectrodes regarding to resolution, signal quality, intracellular access, and fabrication flexibility. And last, we discuss the challenges of current *in vitro* nanoelectrode platforms from the system level of mapping neurons’ electrical dynamics and constructing functional cell-on-chip systems.

Nanoscale Neural Operation

Ionic Operation and Neuronal Computation

Despite the complexity and plasticity of large-scale neural networks, neuronal operations are still governed by the laws of thermodynamics, in which the interactions between chemical and electric potentials are the sole factors that control ionic transports. Various species of cations, such as Na⁺, K⁺, and Ca²⁺, serve as charge carriers for a neuron to generate transmembrane currents. Assisted by the active ion transporters [14], a neuron can maintain constant gradients for each ionic species across its membrane (Table 1). At rest, for each permeable ionic species, its chemical concentration differences across the intracellular and extracellular spaces gives rise to an electric potential difference governed by the Nernst Equation (Equation (1)), which tends to counterbalance the transmembrane concentration gradient. The result is an equilibrium where its chemical and electrical potentials are balanced:

$$E = \frac{RT}{zF} \ln \left(\frac{[\text{ion inside cell}]}{[\text{ion outside cell}]} \right) \quad (1)$$

Table 1. Major charge carrier gradients for typical mammalian neurons

Ion species	Intracellular concentration (mM)	Extracellular concentration (mM)
Na ⁺	10	145
K ⁺	140	5
Mg ²⁺	0.5	2
Ca ²⁺	10 ⁻⁴	2
Cl ⁻	10	110

This Nernst potential is the driving force behind charge carrier transports across the neuronal membrane, and selective ion channels serve as gates to recruit certain ion species for an action potential and to regulate the temporal dynamics of ionic currents. For example, neuronal membrane at rest has very low permeability (non-zero) to Na⁺, thus the cytoplasm and extracellular fluid are nearly isolated systems for Na⁺. Although extracellular Na⁺ are of both higher chemical potential and electric potential, the equilibrium potential of Na⁺ (defined by Equation (1)) has little effect on the resting membrane potential due to such separation. The activation of Na⁺ channels during the early stage of an action potential, once occurs, brings two spaces into a single system where Na⁺ diffuses from the extracellular fluid to the cytoplasm, tending to reach to its equilibrium electrochemical potential. Such alternative electricity is a direct result from the neuron’s contact-separate strategy that uses selective ion channels to switch its charge carriers at different stages of an action potential.

At the cellular level, a single neuron is an independent computational unit and the generation of action potentials is just the result of its computation process. The post-synaptic potentials (PSPs) from distal dendrites, either excitatory or inhibitory, are integrated at the neuronal soma that determines if an action potential will be fired or not (Fig. 1a) [15]. Unlike the digital all-or-none feature of action potentials, these synaptic inputs are analog signals with different amplitudes and durations (Fig. 1b) [16]. More importantly, because of neurite migration and synaptic plasticity, PSPs are both spatial and temporal variant. Taking into account the non-uniform distributions of ion channels, these unique characteristics of neurons will certainly require an electrophysiological platform with capability of high-resolution, long-term, and seamless recording/stimulation, if we want to govern the detailed neuronal dynamics.

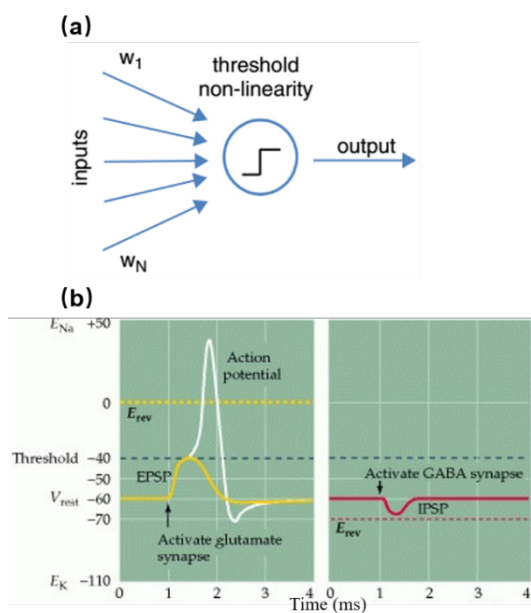


Fig. 1. Neuronal computation process and subthreshold synaptic inputs. (a) The classic McCulloch-Pitts neuron performs a weighted sum of its synaptic inputs (each input i is multiplied by a synaptic weight w_i), and then a thresholding operation. Each incoming presynaptic signal produces a PSP at the postsynaptic terminal, which spreads passively to the cell body (spatial summation). The cell body will perform temporal summation of all the PSPs from different synapses. If the resulted average PSP at soma exceeds the potential threshold, an action potential will be fired. This figure has been adapted from ref [15] with permission from Elsevier. (b) Examples of an excitatory post-synaptic potential (EPSP) and an inhibitive post-synaptic potential (IPSP). The reversal potential (dotted line) of an EPSP is more positive than the action potential threshold, increasing the probability of triggering an action potential. For IPSPs, the reversal potential is more negative than threshold, producing inhibitive effect on action potential generation. This figure has been adapted from ref [16] with permission from Sinauer Associates.

Nanoelectrode-Neuron Interface

The recording/stimulation principle of 3D vertical nanoelectrodes is the same as planar MEAs. However, nanoelectrodes' small dimensions and vertical protrusions can bring significant improvement on some critical parameters. The equivalent circuit of a nanoelectrode-neuron interface is shown in Fig. 2. And a comprehensive discussion on recording mechanisms was covered in ref [17]. The nanoelectrode-electrolyte interface is an electrical double layer (EDL) of capacitive nature. Electrical activities of local membrane, in the form of transmembrane ionic current, causes charge redistribution at the EDL. The electric potential variation caused by such charge redistribution is recorded by the amplifying circuits. Because cell membrane spontaneously wraps around the nano-protrusions (like endocytosis), the resulted tight adhesion can greatly reduce the ionic cleft between the electrode and lipid membrane, suppressing the current leakage through the seal resistance R_{seal} . Moreover, the membrane curvature is spontaneously formed without forced insertions,

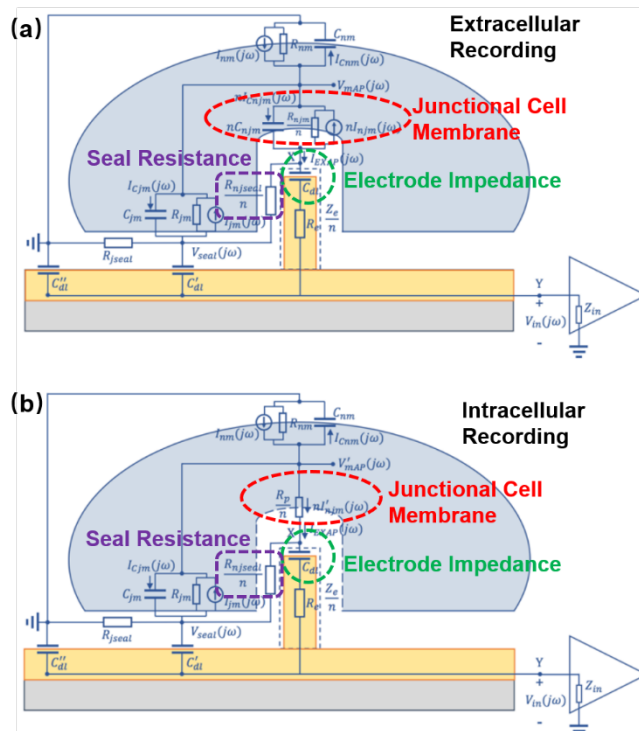


Fig. 2. Transmembrane ionic currents from junctional membrane (red) are the signal sources to be detected by the nanoelectrode. The nanoelectrode-electrolyte interface (green) is a passive capacitor representing the EDL. The adhesion between the electrode and junctional membrane is modeled as a seal resistance (purple), through which current leakage attenuates the amplitude of recorded signals. The equivalent circuits of n interconnected nanoelectrodes are shown. (a) Extracellular recording in which the transmembrane current through local ion channels is the signal source that alters the charge distribution in the EDL. (b) Intra-cellular recording in which the nanoelectrode gains electrical access to the cytoplasm. The internal potential of the neuron connects to the electrode through a pure resistor with its resistance determined by the pore size in the membrane (see *Intracellular Access Through Membrane Poration*). These figures have been adapted from ref. 17 with permission from IOP Publishing.

thus imposing minimum invasiveness and damage to the neuron. Since the junctional area is also at nanoscale, the signal source from the neuronal membrane is highly localized, allowing for the recovery of spatial distribution of ion channels and membrane properties.

Qualitative Breakthroughs by Nano Probes

Even for animals with seemingly simplest behaviors, there might be a rather complicated nervous system functioning behind. In contrast with the rapid development on solid-state electronics that integrates billions of transistors per chip, it took decades for scientists to resolve the complete connectivity of *C. elegans*'s nervous system, an invertebrate worm with only 280 neurons [18]. As mentioned before, a single neuron is a complex

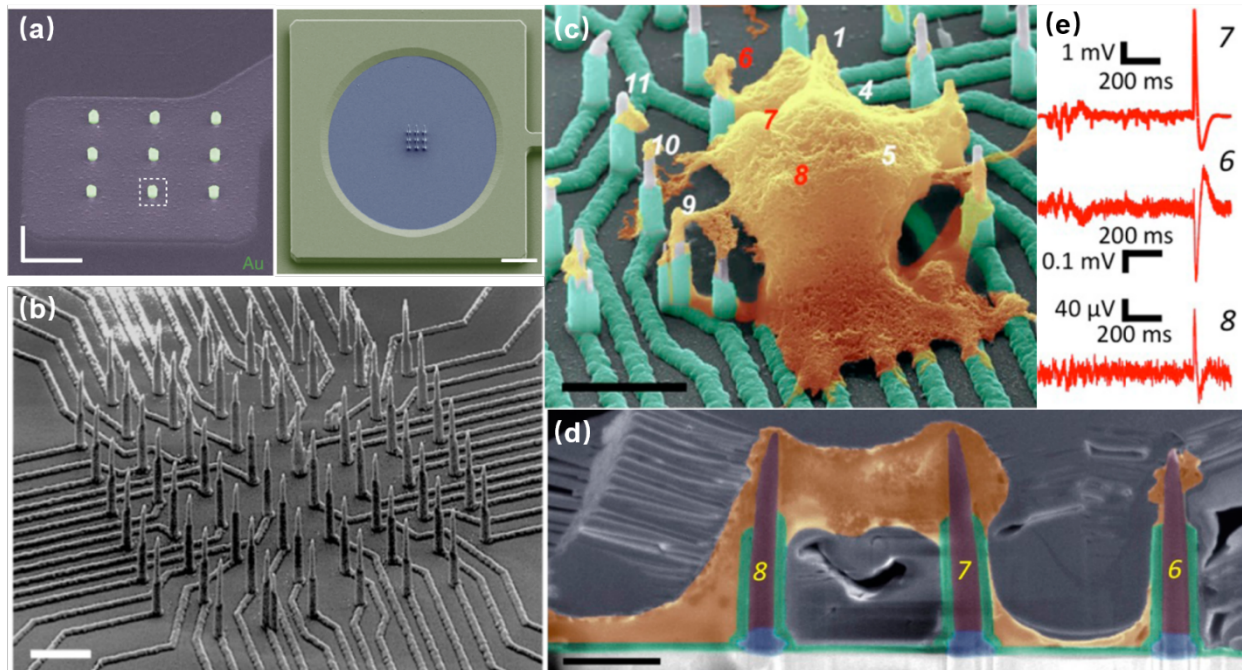


Fig. 3. Interconnected and independent nanoelectrode arrays. (a) Scanning electron microscopy (SEM) images of interconnected nanopillar electrode arrays fabricated on a passivated microelectrode pad. The nanopillars are essentially a combined single recording unit as they are electrically connected by the conductive pad underneath. Left, scale bar: 2 μm ; right, scale bar: 10 μm . These figure have been adapted from ref [21] (left) and [22] (right) with permission from Springer Nature. (b) SEM image of an 8×8 Si nanowire array where each electrode can independently record neuronal signals. Scale bar 3 μm . (c) The nanoelectrode array in (b) interfacing with a neuronal soma at different locations simultaneously. Scale bar: 4 μm . (d) Cross section of nanoelectrode-membrane interface showing intimate membrane engulfment. Scale bar: 2 μm . (e) Variation of signal shapes and amplitudes from different recording sites, allowing for detailed mapping of ionic current distributions. Figure (b-e) have been adapted from ref [23] with permission from American Chemical Society.

computational device that receives inputs from multiple pre-synaptic terminals followed by neurocomputation to produce action potentials of various frequencies. Although the properties of ion channels have been extensively characterized with patch-clamp electrophysiology [19, 20], their non-uniform spatial distribution and time variance make it challenging to decode the computation process. The situation becomes more frustrating for neural networks where the variance of synapse location and time-dependent synaptic strength are involved. Therefore, to sketch the complete picture of nervous system operations, it is imperative, at the fundamental level, to first develop *in vitro* sensors with high resolution and long-term robustness to reveal the electrical activities of single neurons.

Precise Subcellular Interrogation

Fundamentally more advanced than microelectrodes, nanoelectrodes are not only a matter of size-scaling, but a breakthrough regarding to both the quantity and quality of information extracted from cells. MEAs, developed for the

purpose of large scale and parallel neural recordings, are intrinsically limited by their large dimensions and defects at neuronal interface. First of all, with nanoscale ion channels and submicron neurites and synapses, it is difficult for MEAs to pinpoint specific cellular compartments and extract localized information from plasma membrane, as the electrode size of 5–30 μm can only characterize the averaged electrical activities of the attached membrane. As a result, subcellular information reflecting the operation of nanoscale ion channels and submicron neurites and synapses is often attenuated or buried in the signals recorded from larger areas. Second, planar microelectrodes suffer from relatively weak electrode-cell coupling that originates from a 70 – 100 nm cleft between the cell membrane and solid-state probes [24]. Such a cleft, filled with highly conductive electrolyte, attributes to most of the current leakage of the entire recording system [25]. Although the topographical improvement using mushroom protrusions has greatly enhanced the membrane adhesion for cardiomyocytes and Aplysia neurons [26], the inevitable cell

membrane deformation of micrometer size occupies a considerable amount of membrane area, making it difficult to simultaneously extract information from multiple sites of a small mammalian neuron.

Development of nanoelectrodes, especially the vertical nanoprotrusions, allows the probes to integrate with cell membrane at a much finer scale. This intrinsic feature, on one hand, makes it possible for nanoelectrodes to accommodate for the non-uniform distributions of ion channels on the neuronal membrane and to record potentials generated from local ionic currents, which may reveal detailed information of neural computation dynamics [27]. Nanopillars, with diameter of about 100 nm, can interface with only a small portion of the cell membrane, allowing for multiple detections at different sites from a cell. Moreover, nanowire FETs have reached a 10-nm scale, approaching to the dimension of single ion channels [28] (though this device has not achieved extracellular recordings from single ion channels). Early studies often fabricated multiple nanopillars on the same conductive pad, resulting in a loss of individuality as they are electrically interconnected (Fig. 3a). However, the parallel probing advantage of nanoelectrodes has been realized by the breakthrough on high-density and independent nanowire array with a site-to-site spacing of only 750 nm [23], where each nanoprobe, as an independent unit, can acquire high-fidelity electrical signals from its local interface with the neuronal membrane (Fig. 3b). Such submicron-scale information from different sites (Fig. 3cd), combined together, will be valuable for mapping the electrical properties of cell membrane and to understand the spatial and temporal mechanism of how neuronal signals are generated and transmitted.

It should be noted that nanoscale resolution discussed above is limited to extracellular recordings because the potential change of electrical double layer relies on transmembrane current. Once electrodes gain intracellular access, the recorded signals will reflect intracellular potentials that is affected by space constant of cellular compartments.

Enhancement of Seal Resistance

The spontaneous membrane engulfment around nanoelectrodes provides an excellent seal for recording subthreshold membrane potentials. Various studies have characterized the plasma membrane deformation on vertical nanoprotrusions using fluorescence and electron microscopic techniques (Fig. 4a). Although the value of cleft thickness has shown substantial variance among devices, from less than 5 nm to 18 nm [29, 30], it is still no doubt that their membrane attachment are much tighter than that of planar microelectrodes (i.e., a 70 nm – 100 nm cleft), giving rise to a seal resistance of 80 M Ω [29] to 500 M Ω [22], which is more than two orders of magnitude enhancement. Besides the morphologically tight adhesion, the membrane curvature caused by vertical nano-protrusions may also induce aggregation of ion channels, increasing the local ionic currents [31, 32].

Further, treated by hydrophobic bands, nanopillars can even enhance the seal resistance to the G Ω range that is

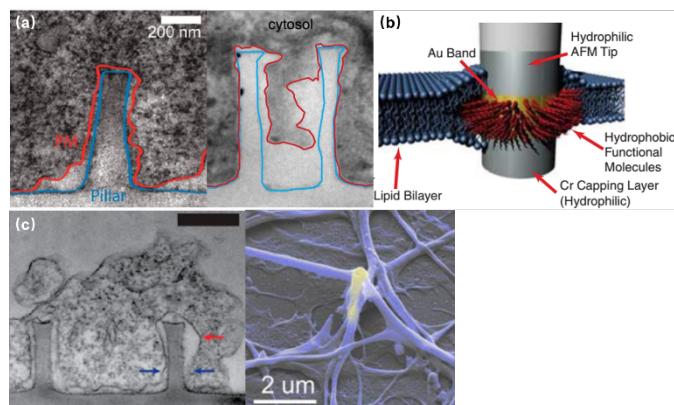


Fig. 4. Seal resistance enhancement by membrane engulfment on 3D nano-protrusions. (a) Left, Transmission electron microscopy (TEM) image of the vertical cross-section of the intimate cell-nanopillar interface. The blue line indicates the border of nanopillar and red line indicates cell's plasma membrane. This figure has been adapted from ref [29] with permission from American Chemical Society. Right, TEM vertical cross-section a cardiomyocyte growing on top of a quartz nanotube showing that the bottom plasma membrane protruded into the nanotube. This figure has been adapted from ref [21] with permission from Springer Nature. (b) Nanopillar coated with hydrophobic band for tight G Ω seal. The 5-10 nm hydrophobic band is self-assembled from butanethiol on Au band. The interactions between the hydrophobic band and cell membrane core produces a tight seal impermeable to charged ions, similar to the behavior of membrane proteins. This figure has been adapted from ref [34] with permission from National Academy of Sciences. (c) Left, vertical cross-section of a large neurite engulfing nanopillars. Red arrows marked a cavity formed on the upper half of the nanopillar, while blue arrows pointed out where the neurite sealed tightly at the bottom of the nanopillar. Scale bar 500 nm. This figure has been adapted from ref [29] with permission from American Chemical Society. Right, SEM image of neuronal processes enveloping a gold plasmonic 3D nanoelectrode. This figure has been adapted from ref [37] with permission from American Chemical Society.

comparable to the patch-clamp seals (Fig. 4b) [33, 34]. Despite the increased electrode impedance caused by the reduced surface area, the improvement of membrane-electrode seal clearly overweighs the sacrifice of electrode impedance, which has been proved through both theoretical study [25] and electrophysiological tests [21-23, 35, 36]. More importantly, membrane engulfment was also observed at large neurites that are difficult to access by patch-clamps and microelectrode arrays (Fig. 4c) [29], providing a promise for parallelly monitoring dendrites, axons, pre- and post-synaptic terminals as these compartments play more significant roles than the soma regarding to neural network plasticity.

Intracellular Access through Membrane Poration

Membrane poration can be conveniently applied to nanoelectrodes to directly record from cytoplasm with higher accuracy and less invasiveness compared to patch clamps and MEAs. By penetrating cell membrane either spontaneously or artificially, intracellular signals will pass through a resistive interface to nanoelectrodes, rather than being filtered by the

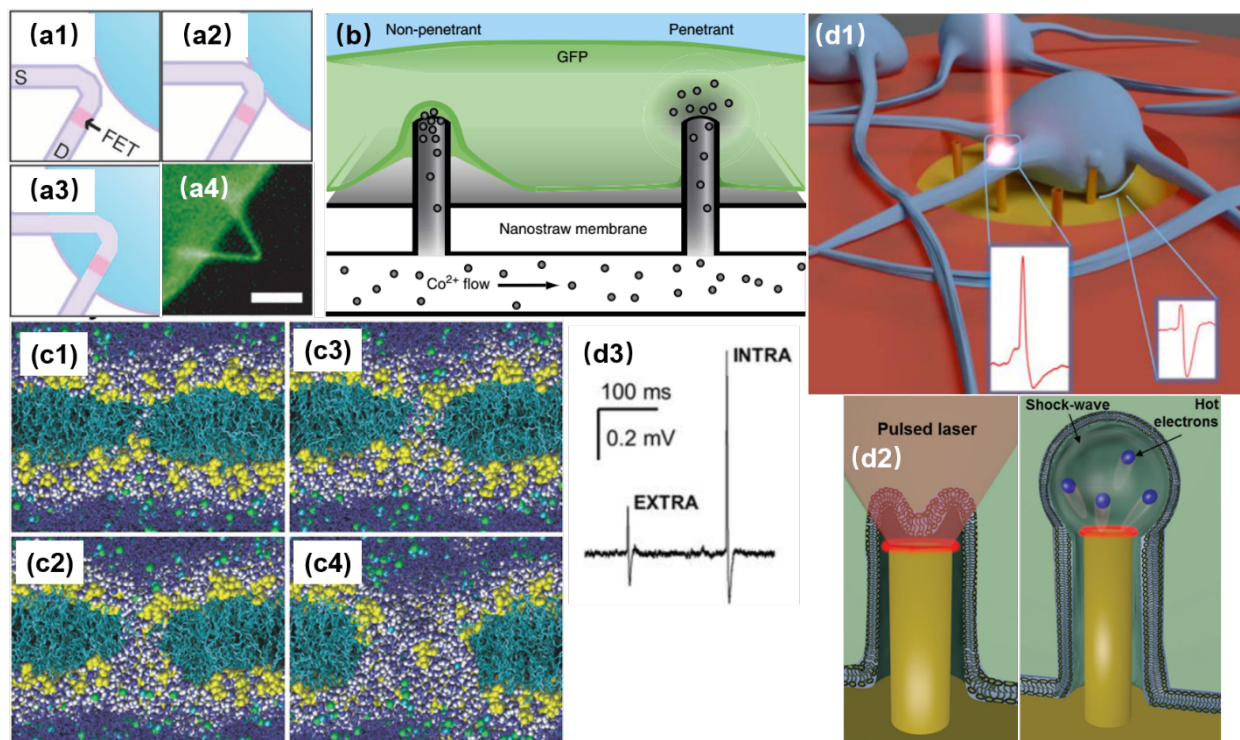


Fig. 5. Intracellular access through localized membrane poration. (a1-a3) Schematics of phospholipid-coated Si nanowire field-effect transistor (FET) probe being inserting into a cell. The process is similar to endocytosis because of the lipid coating and nanoscale dimension. (a4) False-color fluorescence image of a lipid-coated nanowire probe. Scale bar 5 μm . These figures have been adapted from ref [38] with permission from AAAS. (b) Spontaneous membrane penetration by vertical nanostraws where ions can be delivered into cells' cytoplasm through nanostraws' hollow tunnel. This figure has been adapted from ref [40] with permission from Springer Nature. (c) Simulation of electroporation process. The lipid headgroups are shown in yellow, the chains in cyan, chloride ions space filling in green, sodium ions in cyan; water is shown as dark blue and white space filling in the interface region and the pore, as dark blue bonds elsewhere. This figure has been adapted from ref [41] with permission from BioMed Central Ltd. (d1) Schematic of plasmonic optoporation platform for neurons cultured on 3D nanoelectrodes. Low-power laser beams can selectively induce plasmonic effect at individual electrodes to open pores at specific locations. This figure has been adapted from ref [37] with permission from American Chemical Society. (d2) The mechanism of plasmonic membrane poration. Hot electrons excited by laser irradiation induce a mechanical shock wave in water, rupturing the cell membrane. This figure has been adapted from ref [42] with permission from Wiley. (d3) Recorded electric signals before (EXTRA) and after (INTRA) membrane poration. The significantly enhanced signal amplitude and the intracellular-like signal shape indicate that electrode has gain intracellular access after poration. This figure has been adapted from ref [37] with permission from American Chemical Society.

membrane capacitance (Fig. 2b). Also, due to the rather large dimensions of pore openings compared to leaky K^+ channels, the access resistance is significantly lowered, yielding a high signal-to-noise ratio (Fig. 5d3). Unlike the invasive sharp electrodes that often leads to cell death after impalement, vertical nanostructures impose little damage to the lipid membrane. The sub-100 nm dimension and high aspect ratio of the nanostructures induce endocytosis, allowing them to fuse into cells (Fig. 5a) [38]. With biomimetic surface modifications [38, 39] or hydrophobic coatings [34], the fluid leakage between cytoplasm and extracellular medium can also be reduced

significantly, making nanoscale penetration suitable for repeatable intracellular access over long-term recordings.

Spontaneous membrane penetration enabled by vertical nanoprotusions was observed and widely applied in delivering biomolecules into the cytoplasm (Fig. 5b). Without external forces such as centrifuging or manual penetration, the high aspect-ratio of vertical nanowires can induce penetration of cell membrane by gravity or adhesive force driven internalization after cell plating [43, 44], which was reported for various cell lines, primary neurons, fibroblasts, and immune cells [45-50]. Theoretically, for nanoelectrode recordings, spontaneous

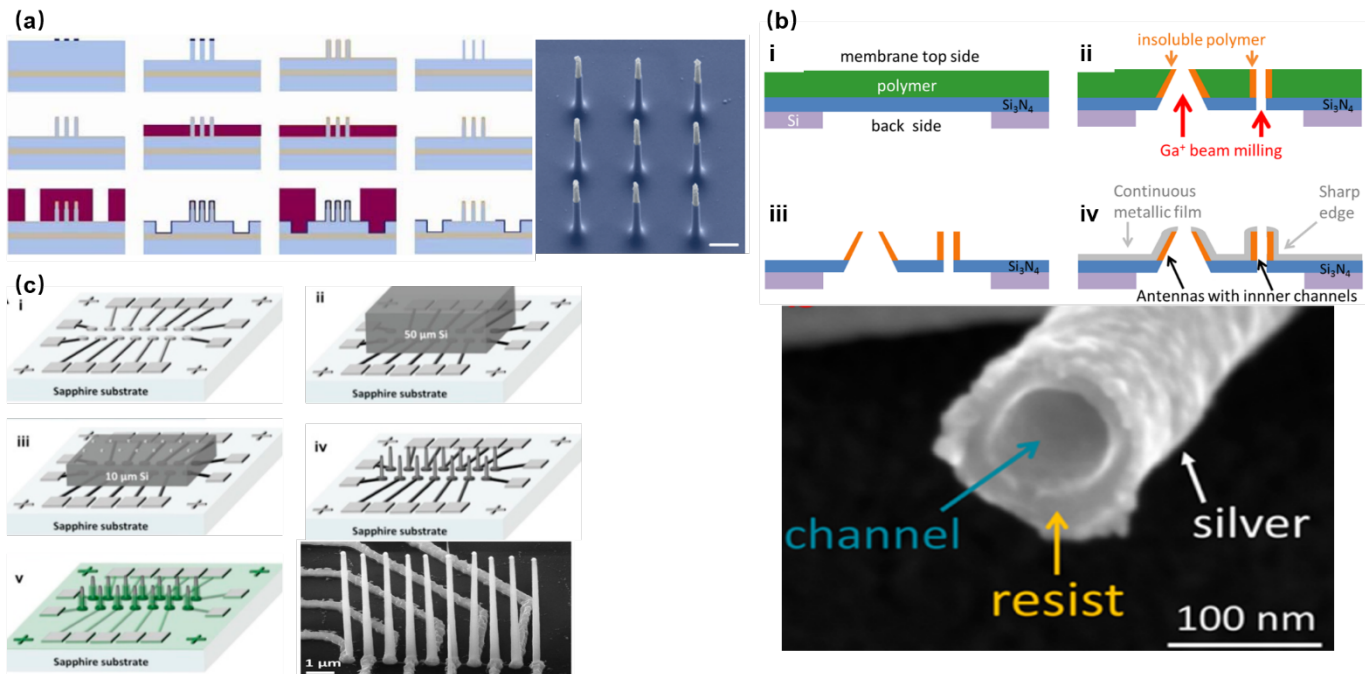


Fig. 6. Top-down fabrication of vertical nanoelectrodes. (a) Si nanowires from oxide thinning and wet etching. The diameter of Si nanowire is 600 nm after lithography and etching. The following thermal oxidation transforms Si to SiO₂. After etching the SiO₂, the nanowire diameter is reduced to 150 nm. This figure has been adapted from ref [22] with permission from Springer Nature. (b) Metal nanotubes from secondary electron FIB milling. Ga⁺ beam is used to define the hollow structures from the backside of Si₃N₄ substrate. Secondary electrons from Ga⁺-polymer interactions exposes the nearby resist, and the high electron doses and the resist heating will turn the resist tone from positive to negative. Thus, the exposed structures stay insoluble during developing, serving as cores for the metal coatings afterwards. This figure has been adapted from ref [52] with permission from American Chemical Society. (c) High-throughput electrode fabrication from thermal wafer bonding, allowing for individual nanowires registered precisely over underlying metal leads. Conventional lithography of Ni layer first defines electrode leads, wirings, and contact pads. A thin Si wafer is then thermally bonded to the Ni layer through nickel silicidation at 400 °C (NiSi formed), followed by e-beam lithography and reactive ion etching on Si to produce the vertical nanoelectrodes. This figure has been adapted from ref [23] with permission from American Chemical Society.

intracellular access has the advantage of stable electrode-neuron interface in which internalized electrodes can maintain their cytoplasm access for a long period of time [40]. Moreover, excluding external forces will reduce the probability of cell damages. However, the performance of this approach has not yet met the requirements of parallel intracellular electrophysiology. The bottleneck lies at the unclear penetration mechanism and low penetration rate of nanowires. Although surface modifications with cell adhesion molecules (CAMs) or cell penetrating pipettes (CPPs) have enhanced the internalization efficiency to 15% [44, 51], it is still not affordable for neuronal recordings since a nanoelectrode array has much fewer probes than relatively simple drug delivery platforms. In addition, a systematic study using nanopillars, nanocones, and sharp nanopillars has revealed that vertical nanostructures spontaneously penetrate the cellular membrane to form a

steady intracellular coupling only in rare cases, and suggested that most of spontaneous penetrations might occur only during the initial hours of cell plating with membrane reseal afterwards [53]. Therefore, it is important to address the robustness issue from both the mechanism and application aspects before spontaneous poration can be exploited further for nano neural electrodes.

On the other hand, artificially induced membrane porations through electrical and optical approaches have been well applied to intracellular recordings. In electroporation, cell membrane can be ruptured under a strong electric field applied at the nanoelectrode tip, allowing for significant improvement on signal amplitude and intracellular-like shapes. The mechanism of this process was investigated by computer simulations. Specifically, water defects, caused by the interaction of water dipoles with the electric field gradient at

the water/lipid interface, are significantly promoted by the external electric fields. As a result, water can penetrate the lipid bilayer from both sides, leading to pore formation (Fig. 5c) [41]. However, since electroporation has to be conducted by the same electrodes for recordings, the switching between pulse injection and recording modes will inevitably result in a blind recording period caused by overcharging. Additionally, the number, size [21, 54], and distribution of membrane pores from electroporation are difficult to predict and characterize [55]. To address these issues, the combination of vertical nanoelectrodes and plasmonic optoporation was developed for opening transient pores at the tips of nanopillars (Fig. 5d1) [37]. Upon irradiation of laser pulses, the Au surface of nanoelectrode generates highly energetic electrons (hot electrons) into water conduction band, which induce a chain reaction of photon absorption and the release of more hot electrons. Eventually, water molecules are accelerated by hot electron impacts, producing a mechanical shock wave that ruptures the cell membrane (Fig. 5d2) [42]. So far, the electrode material has been limited to Au due to its low energy threshold (3.7 – 2.2 eV) for hot electron excitation [42, 56] at solid-water interface. Comparing to electroporation, this approach also has the advantage of localized pore formation, in addition to continuous recording. Because of its essence of mechanical nanoshockwaves, plasmonic optoporation is likely to produce single pores that are highly localized and easier to modulate. Considering that the lipid membrane reseals after poration, a single and localized pore could make the recorded signals with better fidelity and consistency than a group of sparsely distributed pores. This might also attribute to the prolonged period of intracellular access of up to 80 min [37], as it takes more time for the cell membrane to reseal a large pore than many small pores.

For both electroporation and optoporation, the recording window is relatively short (10–80 min, depending on the poration method and parameters). However, nanoelectrode penetration is a highly local process that impacts little on adjacent membrane as well as seal resistance. In fact, the cell membrane spontaneous reseals after the recording window. Thus, the poration could be repeatedly performed (once several hours) over a long-term cell culture. Although this repeated sampling is not a continuous recording, considering that neurons' long term plasticity (learning and memory) is a much slower process, repeated intracellular access with nanoelectrodes still holds great promise for studying long-term neural network dynamics.

Fabrication of Nanoelectrodes

Most substrate-bound vertical nanoelectrodes with diameters of 100 – 200 nm can be either fabricated top-down from bulk materials or bottom-up through crystal growth or deposition. So far, the fabrication techniques have been developed for only doped semiconductors (Si) and noble metals (Pt, Au) due to their compatibility with photo- and e-beam lithography as well as chemical and physical etching. The top-down process has been widely used for metal-coated semiconductor nanopillars lithography was first applied to

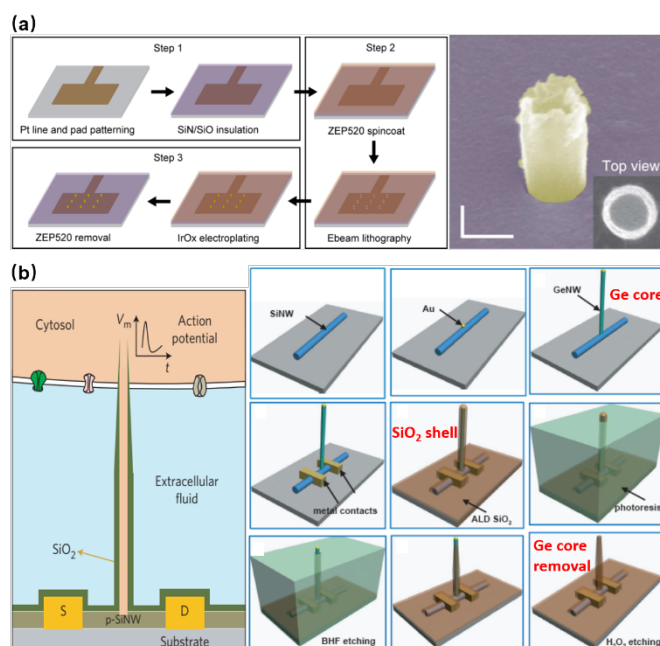


Fig. 7. Bottom-up fabrication of vertical nanoelectrodes. (a) IrOx nanoelectrodes from electrochemical deposition. IrOx nanoprotusions are electroplated on the pre-defined Pt nano patterns. This figure has been adapted from ref [21] with permission from Springer Nature. (b) Schematic, fabrication, and SEM image of Si nanowire FETs from vapor-liquid-solid crystal growth. The inner core of the vertical nanotube is Ge nanowire grown through VLS on a 100-nm Au nanodot (produced by lithography on a lying-down Si nanowire). The entire device is then uniformly coated with SiO₂ to form the outer shell of the nanotube. Finally, the Ge core is selectively removed by H₂O₂, yielding the hollow structure where ionic fluid makes contact with the lying-down Si nanowire. Therefore, Intracellular electric signals (as Gate voltage) are able to modulate the current passing through the Si nanowire (from Source to Drain). This figure has been adapted from ref [59] with permission from Springer Nature.

define the diameters of electrodes on photoresists, followed by reactive ion etching to remove uncovered material and leave out vertical nanostructures of high aspect-ratios. Additionally, since the top-down approach is a well-established process in dealing with semiconductors, it promotes innovative improvements to achieve various electrode geometries, smaller diameters, and higher densities. For example, the diameter of Si nanowire electrodes was reduced from 600 nm to 150 nm by thermal oxide thinning, based on that Si can be thermally oxidized to SiO₂ which can then be selectively etched by HF (Fig. 6a) [22]. Fabrication of hollow nanotubes exploited the tone-inversion of photoresists by secondary electrons during focused ion-beam (FIB) milling (Fig. 6b), resulting in a cylinder wall that cannot be removed by developers [52]. Plus, the density of independent nanoelectrodes was greatly enhanced by thermally bonding a Si wafer onto patterned metal leads before e-beam lithography and plasma etching (Fig. 6c) [23].

Noble metals of Pt and Au have excelled in microelectrodes because of their inertness in biological fluids and excellent conductivity, rendering robust neural interfaces for long-term sensing. For nanoelectrodes, however, metals are highly

resistant to plasma etching, and it would be expensive and unreliable to use conventional lift-off process for high-aspect-ratio protrusions with 1–3 μm height. Therefore, the bottom-up approach by selective deposition has been mostly adopted for metal nanoelectrodes. Specifically, nanoscale holes can be milled on a layer of photoresist by e-beam lithography, followed by electrochemical deposition or focused ion beam (FIB)-assisted deposition to create the protrusion structure (Fig. 7a) [21]. In comparison to semiconductor-based processes, the bottom-up deposition involves much fewer steps that greatly reduces fabrication failures. Moreover, it is insensitive to substrates so that transparent glass and quartz can conveniently serve as substrates for cell observation under inverted microscopes. However, because of the limited maneuverability of noble metals at nanoscale, bottom-up fabricated electrodes are often pillar-shaped without the sharpened tips (like the Si electrodes), which may more or less affect the cell membrane-electrode interface due to their restrained bending ability under the pulling force from the cell membrane and the larger curvature at electrode tips [57]. Another factor that makes semiconductor electrodes more popular is the compatibility with CMOS technologies that integrate on-chip amplifiers at the vicinity of electrode probes, significantly reducing the amplitude loss by eliminating the stray capacitance [58].

Besides electrode-based nanoprobe, bottom-up crystal growth through vapor-liquid-solid (VLS) deposition is also the most critical process in the fabrication of nanowire field-effect transistors (NWFETs) [38, 59–61]. Composed of three terminals: source (S), drain (D), and gate (G), an FET's charge carrier density in the S-D channel are modulated by the voltage applied on the gate, thus resulting in a conductance controlled by the gate. During neural recordings, the alternating electric potential from a neuron serves as the gate voltage that modulates the S-D current (Fig. 7b). The original neuronal potentials can then be recovered by fitting this current into the known transconductance characteristics of the FET. Despite its unique structure, the working principle of NWFETs is not essentially different from vertical nanoelectrodes, as both devices operate upon charge redistribution at the solid-electrolyte interface. Instead of transmitting signals to amplifiers through metallic wirings, the FETs function as amplifying units integrated directly with the double layer capacitance, thus eliminating the stray capacitance and wiring resistance that compromise the signal-to-noise ratio [58].

Dilemmas towards Seamless Neural-Chip Interface

In-Situ Characterization of Electrode-Neuron Seal

Neuronal signals acquired by nanoelectrodes are strongly affected by the seal resistance R_{seal} due to high electrode impedances. More importantly, it is imperative to measure R_{seal} for each electrode in order to recover a neuron's actual electrical activities. Indeed, the tight adhesion between cell membrane and vertical nanostructures yielded detectable

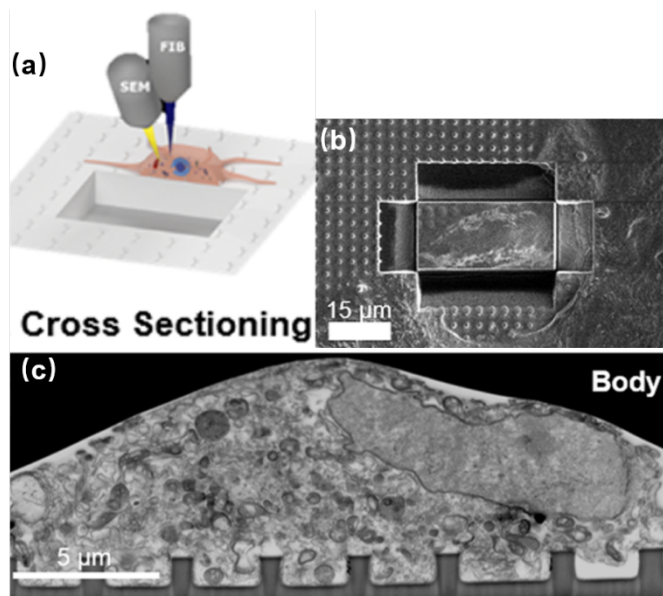


Fig. 8. (a) Schematics and (b) experimental results of using FIB milling to cut trenches through the cell and the substrate and open up the interface. The FIB provides high-energy Ga^+ beam to cut through the sample and open up a vertical surface. Meanwhile, SEM conducts *in-situ* imaging of the cross section. (c) FIB-SEM image of the neuronal body on a line of nanopillars. These figures have been adapted from ref [63] with permission from American Chemical Society.

intracellular-like signals after membrane poration. However, interfacing with different neuronal compartments of different dimensions, each electrode will possess a unique R_{seal} , causing substantial variance across electrodes. Moreover, neuronal migration may also attribute to the time-variation of R_{seal} . Apparently, if this critical parameter is not available or well characterized, the recorded data will lost its quantitative information.

A variety of methods have been developed to topographically characterize the membrane-surface gaps, which have been comprehensively covered in Ref. [62]. In general, imaging of highest resolution can be achieved through transmission electron microscopy (TEM) where the cell-on-chip devices are thin-sliced before observation (Fig. 4a) [29, 30]. Alternatively, FIB and scanning electron microscopy (FIB/SEM) can target the biointerface at any desired locations through FIB milling (Fig. 8) [63, 64], which greatly improves the technical flexibility over TEM. However, electron microscopy is a destructive process that can only be conducted at the final stage, as the cells have to be killed during sample preparation. On the other hand, live cell imaging such as fluorescent confocal [65, 66] and curvature-sensing proteins [67–70], can qualitatively reveal the membrane engulfment around nanopillars but could not provide quantitative information on the seal resistance.

Despite the lack of techniques for *in-situ* characterization, membrane-surface seal can still be estimated from electric models. However, the values of R_{seal} showed rather significant dispute among different devices, from tens of $\text{M}\Omega$ to $\text{G}\Omega$. Typically, these estimations were obtained by fitting the

recorded waveforms into the electric model of electrode-neuron interface [23, 35]. For example, in an equivalent circuit model, the electrode impedance, stray capacitance, and amplifier input impedance can be either measured or estimated with reasonable accuracy. Given the signals generated by the target cell, R_{seal} can be estimated by sweeping until the simulation results fit well with the recorded data. However, in order to calculate R_{seal} , the neuronal signal sources, which are supposed to be revealed by nanoelectrodes, are assumptively predefined. This approach might work well when recording action potentials with known waveforms. But when it comes to subthreshold signals from neurites, it will no longer be able to as there is no predefined signals available to calibrate R_{seal} . Therefore, for nanoelectrodes to work independently as robust neural interfaces, it is important to develop *in-situ* measurement approaches.

Bidirectional Recording and Modulation

High-fidelity bidirectional communication is critical for accurate and intelligent cell-on-chip systems and brain-machine interfaces, as neural probes should not only discover neural activities but also exert control over neural networks. For nanoelectrodes based on solid-electrolyte interface, the charge transport of capacitive nature makes the recording quality more vulnerable to poor seal resistance, and suffers from signal distortion due to phase shift. For a typical nanoelectrode with 1 pF surface capacitance, its impedance is about 150 M Ω for 1 kHz signals, and will increase significantly for slower changing signals. Since such an impedance is comparable or higher than the seal resistance (100 – 500 M Ω), both the amplitude and shape of recorded signals will be affected substantially by the electrode-membrane seal. Moreover, low-frequency field potentials may have important linkage to brain's perception, motion, and memory [71, 72], but will be severely attenuated by nanoelectrodes' high impedance. Additionally, considering the missing approach to accurately measure seal resistances *in situ*, the fidelity of acquired data has to be put under question.

On the other hand, this issue became more problematic for neural modulation purposes. The small surface area of nanoelectrodes results in an extremely low charge delivery capacity, which might be able to inject miniature post-synaptic currents (mPSCs, 10-20 pA amplitude, 10 ms duration [73]) but not evoked excitatory post-synaptic currents simulating presynaptic spikes (eEPSCs, 0.1-0.2 nA amplitude, more than 50-ms duration [74]). Although larger current injection can be realized by breaking into the Faradic regime [22], the electrochemical reactions will inevitably cause electrode degradation and even water electrolysis for polarizable electrodes like Au or Pt. Additionally, the slow recovery/discharging process after stimulation makes it difficult to immediately switch an electrode from stimulation to recording.

Direct ionic access with resistive nature has the potential to clear these intrinsic defects from solid-electrolyte interfaces. For example, conventional electrophysiological technology using fluid-filled micropipettes are capable of both signal acquisition and current injection at the same time. Despite its

major drawback of destructive membrane penetration, fluid diffusion, and limited parallel access, the direct ionic interface established between fluid-filled micropipettes and neuronal cytoplasm allows them to yield reliable, high-fidelity, and consistent results, due to their low access resistance (about 25 M Ω for sharp electrodes with a 10 nm tip). More importantly, combined with non-polarizable Ag/AgCl electrodes and Wheatstone Bridge circuit, a micropipette electrode at current-clamp mode is able to implement simultaneous stimulation and recording [75].

Such a concept was partially realized by the nanotube intracellular probes made from chemically grown Si nanowires (Fig. 7b) [28, 59]. With FETs integrated at the bottom of nanotube, this bioelectronic probe provided high-resolution intracellular mapping of electrogenic cells. Yet the using of FETs as interface also precluded the compatibility for current injections. Surprisingly, the breakthrough in nanoscale ionic neural interface occurred mainly in the field of drug delivery, where vertical nanostraws (hollow nanotubes) impaled cell membrane, allowing for the diffusion of molecules into the cytoplasm (Fig. 5b) [40, 76-80]. Specifically designed for drug delivery, nanostraws in these devices are not individually addressable. In addition, the unclear mechanism of spontaneous membrane penetration gives rise to unstable and low percentage of cytoplasm access. Despite their current shortcomings, the success of nanostraw fluid platforms and nanotube FETs still demonstrated that the ionic nano-neural electrophysiology is fundamentally and technically feasible, providing a great promise for future engineering improvement.

Rational Alignment with Neurites and Synapses

Despite the extraordinary signal acquisition performance of 3D nanoelectrodes, these devices should not be limited within the vision of capturing intracellular-like signals or gaining larger amplitudes, and a lot of engineering needs to be applied to fully exploit their potential of precise and parallel neural interface. If we treat a neuron as a system, its dendrites, axons, and synapses are where the ionic current inputs, outputs, and intercellular signal passage take place. Especially, it is the temporal and spatial diversity of chemical synapses that gives rise to the plasticity of neural networks. Both excitatory and inhibitory synapses can exist on the same neuron, and the synaptic strength can be influenced by Hebbian plasticity [81] or heterosynaptic modulation [82]. These critical but small neuronal features at 1-2 μ m dimensions, though having been qualitatively studied using biological approaches [83], still need to be quantified by electrophysiology in order to establish interface with modern electronic chips. Li et al. have demonstrated that carbon fiber nanometric electrodes (CFNEs) can accurately access individual synapses and monitor the dynamics of neurotransmitter fluxes [84] (Fig. 9), which suggested that nanoelectrodes hold great promises in hacking the neurites and synapses. However, CFNEs are mounted on glass micropipettes operated through the conventional patch-clamp setup, eliminating its potential for large-scale parallel recording. For vertical nanoelectrode arrays, however, the

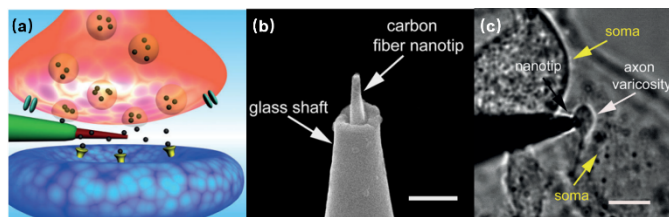


Fig. 9. Carbon fiber nanoelectrode mounted on a glass micropipette for sensing synaptic events. (a) Schematic of a nanoelectrode tip inside a synapse. (b) SEM image of the CFNE. Carbon fiber etched down to 50–200 nm (diameter) is inserted into a pre-pulled glass micropipette. Scale bar: 1 μm . (c) Bright-field microscopy image showing the nanotip inside a synapse between a varicosity of a superior cervical ganglion (SCG) sympathetic neuron and the soma of another SCG neuron. Scale bar: 5 μm . These figures have been adapted from ref [84] with permission from Wiley.

question still opens on how to precisely access the critical neuronal compartments while maintaining comprehensive coverage of the entire neuron. Therefore, engineering efforts on cell manipulation, neurite guidance, and nanoelectrode alignment are to be expected in the future to functionally integrate nanoelectrode arrays with neuronal circuits.

Conclusions

The advancement of nano neural electrodes is a joint effort from nanofabrication, neuroscience, electronic engineering, and biophysics. Behind this development lies the rationale of matching to the nanoscale neuronal compartments (i.e., local ion channels, synapses, and neurites) that are critical to information processing. Ideally, neural interfaces should be able to selectively monitor the electrical activities of neurons without inducing acute damages or substantially altering the neuron's natural status. For 3D vertical nanoelectrodes, scaling down the electrode sizes to less than 200 nm has caused minimal membrane deformation (relative to the total deformed area) while enabling precise electrical neuronal interfaces at the subcellular level. Arranging the nanoprotusions into individually addressable arrays further opens the possibility of parallel, large-scale neuronal recordings without labor-intensive manipulations.

Besides the rationale of accurate probing, organized vertical nanoelectrode arrays are more prominent over other nanoscale interfaces (such as dispersed nanoparticles and nanowires [85], and lying-down nanowires [86]), because the unique topography of substrate-bound vertical nanostructures addressed two significant barriers towards robust neuron-electronic integration: membrane-electrode seal and reliable intracellular access. The spontaneous membrane engulfment greatly reduced the current leakage through the seal, ensuring a good signal-to-noise ratio. And the membrane poration by electrical or optical approaches can be realized with low power injection, high repeatability, and membrane recovery. Overcoming these fundamental issues has made vertical

nanoelectrodes a promising platform for neuron-chip communications.

Nevertheless, several key challenges still need to be addressed to push this technology further towards functional cell-on-chip systems. As mentioned in the dilemmas, the prerequisite for understanding and decoding neuronal computation from recorded data is the awareness of the recording conditions. The lack of approaches for characterizing the seal resistance *in situ* will inevitably make the recorded signals less trustworthy. On the other hand, the high electrode impedance from the electric double layer capacitance has put an intrinsic limitation for both recording and stimulation purposes, which might be resolved by switching to direct ionic interfaces. Moreover, regarding to device functionality, aligning nanoelectrodes with neurites and synapses needs to be addressed in the future to fully exploit the nanoscale advantages.

Conflicts of interest

There are no conflicts to declare.

Acknowledgements

This work was partially supported by the National Science Foundation through Grant # 1749701 and the Defense Advanced Research Projects Agency through Grant # D17AP00031 of the USA. The views, opinions, and/or findings contained in this article are those of the author and should not be interpreted as representing the official views or policies, either expressed or implied, of the Defense Advanced Research Projects Agency or the Department of Defense.

References

- [1] Zhao Z, Luan L, Wei X, Zhu H, Li X, Lin S, Siegel J J, Chitwood R A and Xie C 2017 Nanoelectronic Coating Enabled Versatile Multifunctional Neural Probes *Nano Letters* **17** 4588–95
- [2] Luan L, Sullender C T, Li X, Zhao Z, Zhu H, Wei X, Xie C and Dunn A K 2018 Nanoelectronics enabled chronic multimodal neural platform in a mouse ischemic model *Journal of neuroscience methods* **295** 68–76
- [3] Wei X, Luan L, Zhao Z, Li X, Zhu H, Potnis O and Xie C 2018 Nanofabricated Ultraflexible Electrode Arrays for High-Density Intracortical Recording *Advanced Science* **5** 1700625
- [4] Zhao Z, Li X, He F, Wei X, Lin S and Xie C 2019 Parallel, minimally-invasive implantation of ultra-flexible neural electrode arrays *Journal of neural engineering* **16** 035001
- [5] Luan L, Wei X, Zhao Z, Siegel J J, Potnis O, Tuppen C A, Lin S, Kazmi S, Fowler R A, Holloway S, Dunn A K, Chitwood R A and Xie C 2017 Ultraflexible nanoelectronic probes form reliable, glial scar-free neural integration *Science Advances* **3** e1601966

- [6] Kleinfeld D, Luan L, Mitra P P, Robinson J T, Sarpeshkar R, Shepard K, Xie C and Harris T D 2019 Can One Concurrently Record Electrical Spikes from Every Neuron in a Mammalian Brain? *Neuron* **103** 1005-15
- [7] Robinson J T, Pohlmeier E, Gather M C, Kemere C, Kitching J E, Malliaras G G, Marblestone A, Shepard K L, Stieglitz T and Xie C 2019 Developing Next-Generation Brain Sensing Technologies—A Review *IEEE Sensors Journal* **19** 10163-75
- [8] Jiang Y and Tian B 2018 Inorganic semiconductor biointerfaces *Nature Reviews Materials* **3** 473-90
- [9] Marino A, Arai S, Hou Y, Sinibaldi E, Pellegrino M, Chang Y-T, Mazzolai B, Mattoli V, Suzuki M and Ciofani G 2015 Piezoelectric Nanoparticle-Assisted Wireless Neuronal Stimulation *ACS Nano* **9** 7678-89
- [10] Eom K, Kim J, Choi J M, Kang T, Chang J W, Byun K M, Jun S B and Kim S J 2014 Enhanced Infrared Neural Stimulation using Localized Surface Plasmon Resonance of Gold Nanorods *Small* **10** 3853-7
- [11] Paviolo C, McArthur S L and Stoddart P R 2015 Gold Nanorod-assisted Optical Stimulation of Neuronal Cells *Journal of visualized experiments : JoVE* 98
- [12] Wang Y and Guo L 2016 Nanomaterial-Enabled Neural Stimulation *Frontiers in Neuroscience* **10**
- [13] Carvalho-de-Souza J L, Treger J S, Dang B, Kent S B, Pepperberg D R and Bezanilla F 2015 Photosensitivity of neurons enabled by cell-targeted gold nanoparticles *Neuron* **86** 207-17
- [14] Feher J 2017 *Quantitative Human Physiology (Second Edition)*, ed J Feher (Boston: Academic Press) pp 170-81
- [15] Brunel N, Hakim V and Richardson M J E 2014 Single neuron dynamics and computation *Current Opinion in Neurobiology* **25** 149-55
- [16] Purves D A G, Fitzpatrick D 2001 *Neuroscience. 2nd edition.*, (Sunderland (MA): Sinauer Associates)
- [17] Liang G 2019 On neural recording using nanoprotrusion electrodes *Journal of neural engineering*, doi: 10.1088/1741-2552/ab51de.
- [18] Cook S J, Jarrell T A, Brittin C A, Wang Y, Bloniarz A E, Yakovlev M A, Nguyen K C Q, Tang L T H, Bayer E A, Duerr J S, Bülow H E, Hobert O, Hall D H and Emmons S W 2019 Whole-animal connectomes of both *Caenorhabditis elegans* sexes *Nature* **571** 63-71
- [19] Dunlop J, Bowlby M, Peri R, Vasilyev D and Arias R 2008 High-throughput electrophysiology: an emerging paradigm for ion-channel screening and physiology *Nature Reviews Drug Discovery* **7** 358-68
- [20] Gutman G A, Chandy K G, Grissmer S, Lazdunski M, McKinnon D, Pardo L A, Robertson G A, Rudy B, Sanguinetti M C, Stuhmer W and Wang X 2005 International Union of Pharmacology. LIII. Nomenclature and molecular relationships of voltage-gated potassium channels *Pharmacological reviews* **57** 473-508
- [21] Lin Z C, Xie C, Osakada Y, Cui Y and Cui B 2014 Iridium oxide nanotube electrodes for sensitive and prolonged intracellular measurement of action potentials *Nature Communications* **5** 3206
- [22] Robinson J T, Jorgolli M, Shalek A K, Yoon M-H, Gertner R S and Park H 2012 Vertical nanowire electrode arrays as a scalable platform for intracellular interfacing to neuronal circuits *Nature Nanotechnology* **7** 180-4
- [23] Liu R, Chen R, Elthakeb A T, Lee S H, Hinckley S, Khraiche M L, Scott J, Pre D, Hwang Y, Tanaka A, Ro Y G, Matsushita A K, Dai X, Soci C, Biesmans S, James A, Nogan J, Jungjohann K L, Pete D V, Webb D B, Zou Y, Bang A G and Dayeh S A 2017 High Density Individually Addressable Nanowire Arrays Record Intracellular Activity from Primary Rodent and Human Stem Cell Derived Neurons *Nano Letters* **17** 2757-64
- [24] Joye N, Schmid A and Leblebici Y 2009 Electrical modeling of the cell–electrode interface for recording neural activity from high-density microelectrode arrays *Neurocomputing* **73** 250-9
- [25] Wu Y and Guo L 2018 Enhancement of Intercellular Electrical Synchronization by Conductive Materials in Cardiac Tissue Engineering *IEEE transactions on bio-medical engineering* **65** 264-72
- [26] Hai A, Shappir J and Spira M E 2010 In-cell recordings by extracellular microelectrodes *Nature Methods* **7** 200-2
- [27] Mechler F and Victor J D 2012 Dipole characterization of single neurons from their extracellular action potentials *J Comput Neurosci* **32** 73-100
- [28] Fu T-M, Duan X, Jiang Z, Dai X, Xie P, Cheng Z and Lieber C M 2014 Sub-10-nm intracellular bioelectronic probes from nanowire–nanotube heterostructures *Proceedings of the National Academy of Sciences* **111** 1259-64
- [29] Hanson L, Lin Z C, Xie C, Cui Y and Cui B 2012 Characterization of the Cell–Nanopillar Interface by Transmission Electron Microscopy *Nano Letters* **12** 5815-20
- [30] Mumm F, Beckwith K M, Bonde S, Martinez K L and Sikorski P 2013 A Transparent Nanowire-Based Cell Impalement Device Suitable for Detailed Cell–Nanowire Interaction Studies *Small* **9** 263-72
- [31] Rabieh N, Ojovan S M, Shmoel N, Erez H, Maydan E and Spira M E 2016 On-chip, multisite extracellular and intracellular recordings from primary cultured skeletal myotubes *Scientific reports* **6** 36498
- [32] Shmoel N, Rabieh N, Ojovan S M, Erez H, Maydan E and Spira M E 2016 Multisite electrophysiological recordings by self-assembled loose-patch-like junctions between cultured hippocampal neurons and mushroom-shaped microelectrodes *Scientific reports* **6** 27110
- [33] Verma P and Melosh N A 2010 Gigaohm resistance membrane seals with stealth probe electrodes *Applied Physics Letters* **97** 033704
- [34] Almquist B D and Melosh N A 2010 Fusion of biomimetic stealth probes into lipid bilayer cores *Proceedings of the National Academy of Sciences* **107** 5815-20
- [35] Abbott J, Ye T, Qin L, Jorgolli M, Gertner R S, Ham D and Park H 2017 CMOS nanoelectrode array for all-electrical intracellular electrophysiological imaging *Nature Nanotechnology* **12** 460
- [36] Lee K-Y, Kim I, Kim S-E, Jeong D-W, Kim J-J, Rhim H, Ahn J-P, Park S-H and Choi H-J 2014 Vertical nanowire probes for intracellular signaling of living cells *Nanoscale Research Letters* **9** 56
- [37] Dipalo M, Amin H, Lovato L, Moia F, Caprettini V, Messina G C, Tantussi F, Berdondini L and De Angelis F 2017 Intracellular and Extracellular Recording of Spontaneous Action Potentials in Mammalian Neurons and Cardiac Cells with 3D Plasmonic Nanoelectrodes *Nano Letters* **17** 3932-9

- [38] Tian B, Cohen-Karni T, Qing Q, Duan X, Xie P and Lieber C M 2010 Three-Dimensional, Flexible Nanoscale Field-Effect Transistors as Localized Bioprobes *Science* **329** 830-4
- [39] Qing Q, Jiang Z, Xu L, Gao R, Mai L and Lieber C M 2013 Free-standing kinked nanowire transistor probes for targeted intracellular recording in three dimensions *Nature Nanotechnology* **9** 142
- [40] Xu A M, Aalipour A, Leal-Ortiz S, Mekhdjian A H, Xie X, Dunn A R, Garner C C and Melosh N A 2014 Quantification of nanowire penetration into living cells *Nature Communications* **5** 3613
- [41] Tieleman D P 2004 The molecular basis of electroporation *BMC biochemistry* **5** 10
- [42] Messina G C, Dipalo M, La Rocca R, Zilio P, Caprettini V, Proietti Zaccaria R, Toma A, Tantussi F, Berdondini L and De Angelis F 2015 Spatially, Temporally, and Quantitatively Controlled Delivery of Broad Range of Molecules into Selected Cells through Plasmonic Nanotubes *Advanced Materials* **27** 7145-9
- [43] Shalek A K, Robinson J T, Karp E S, Lee J S, Ahn D-R, Yoon M-H, Sutton A, Jorgolli M, Gertner R S, Gujral T S, MacBeath G, Yang E G and Park H 2010 Vertical silicon nanowires as a universal platform for delivering biomolecules into living cells *Proceedings of the National Academy of Sciences* **107** 1870-5
- [44] Lee J-H, Zhang A, You S S and Lieber C M 2016 Spontaneous Internalization of Cell Penetrating Peptide-Modified Nanowires into Primary Neurons *Nano Letters* **16** 1509-13
- [45] Kim W, Ng J K, Kunitake M E, Conklin B R and Yang P 2007 Interfacing Silicon Nanowires with Mammalian Cells *Journal of the American Chemical Society* **129** 7228-9
- [46] Hällström W, Mårtensson T, Prinz C, Gustavsson P, Montelius L, Samuelson L and Kanje M 2007 Gallium Phosphide Nanowires as a Substrate for Cultured Neurons *Nano Letters* **7** 2960-5
- [47] Jiang K, Fan D, Belabassi Y, Akkaraju G, Montchamp J-L and Coffer J L 2009 Medicinal Surface Modification of Silicon Nanowires: Impact on Calcification and Stromal Cell Proliferation *ACS Applied Materials & Interfaces* **1** 266-9
- [48] Qi S, Yi C, Ji S, Fong C C and Yang M 2009 Cell adhesion and spreading behavior on vertically aligned silicon nanowire arrays *ACS Appl Mater Interfaces* **1** 30-4
- [49] Turner A M, Dowell N, Turner S W, Kam L, Isaacson M, Turner J N, Craighead H G and Shain W 2000 Attachment of astroglial cells to microfabricated pillar arrays of different geometries *Journal of biomedical materials research* **51** 430-41
- [50] Shalek A K, Gaublomme J T, Wang L, Yosef N, Chevrier N, Andersen M S, Robinson J T, Pochet N, Neuberg D, Gertner R S, Amit I, Brown J R, Hacohen N, Regev A, Wu C J and Park H 2012 Nanowire-Mediated Delivery Enables Functional Interrogation of Primary Immune Cells: Application to the Analysis of Chronic Lymphocytic Leukemia *Nano Letters* **12** 6498-504
- [51] Copolovici D M, Langel K, Eriste E and Langel Ü 2014 Cell-Penetrating Peptides: Design, Synthesis, and Applications *ACS Nano* **8** 1972-94
- [52] De Angelis F, Malerba M, Patrini M, Miele E, Das G, Toma A, Zaccaria R P and Di Fabrizio E 2013 3D Hollow Nanostructures as Building Blocks for Multifunctional Plasmonics *Nano Letters* **13** 3553-8
- [53] Dipalo M, McGuire A F, Lou H-Y, Caprettini V, Melle G, Bruno G, Lubrano C, Matino L, Li X, De Angelis F, Cui B and Santoro F 2018 Cells Adhering to 3D Vertical Nanostructures: Cell Membrane Reshaping without Stable Internalization *Nano Letters* **18** 6100-5
- [54] Hai A and Spira M E 2012 On-chip electroporation, membrane repair dynamics and transient in-cell recordings by arrays of gold mushroom-shaped microelectrodes *Lab on a chip* **12** 2865-73
- [55] Abbott J, Ye T, Ham D and Park H 2018 Optimizing Nanoelectrode Arrays for Scalable Intracellular Electrophysiology *Accounts of chemical research* **51** 600-8
- [56] Musumeci F and Pollack G H 2012 Influence of water on the work function of certain metals *Chemical physics letters* **536** 65-7
- [57] Santoro F, Dasgupta S, Schnitker J, Auth T, Neumann E, Panaitov G, Gompper G and Offenhäusser A 2014 Interfacing Electrogenic Cells with 3D Nanoelectrodes: Position, Shape, and Size Matter *ACS Nano* **8** 6713-23
- [58] Spira M E and Hai A 2013 Multi-electrode array technologies for neuroscience and cardiology *Nature Nanotechnology* **8** 83
- [59] Duan X, Gao R, Xie P, Cohen-Karni T, Qing Q, Choe H S, Tian B, Jiang X and Lieber C M 2012 Intracellular recordings of action potentials by an extracellular nanoscale field-effect transistor *Nature Nanotechnology* **7** 174-9
- [60] Cohen-Karni T, Casanova D, Cahoon J F, Qing Q, Bell D C and Lieber C M 2012 Synthetically encoded ultrashort-channel nanowire transistors for fast, pointlike cellular signal detection *Nano Lett* **12** 2639-44
- [61] Gao R, Strehle S, Tian B, Cohen-Karni T, Xie P, Duan X, Qing Q and Lieber C M 2012 Outside Looking In: Nanotube Transistor Intracellular Sensors *Nano Letters* **12** 3329-33
- [62] Lou H Y, Zhao W, Zeng Y and Cui B 2018 The Role of Membrane Curvature in Nanoscale Topography-Induced Intracellular Signaling *Accounts of chemical research* **51** 1046-53
- [63] Santoro F, Zhao W, Joubert L-M, Duan L, Schnitker J, van de Burgt Y, Lou H-Y, Liu B, Salteo A, Cui L, Cui Y and Cui B 2017 Revealing the Cell-Material Interface with Nanometer Resolution by Focused Ion Beam/Scanning Electron Microscopy *ACS Nano* **11** 8320-8
- [64] von Erlach T C, Bertazzo S, Wozniak M A, Horejs C-M, Maynard S A, Attwood S, Robinson B K, Autefage H, Kallepitis C, del Río Hernández A, Chen C S, Goldoni S and Stevens M M 2018 Cell-geometry-dependent changes in plasma membrane order direct stem cell signalling and fate *Nature Materials* **17** 237-42
- [65] Berthing T, Bonde S, Rostgaard K R, Madsen M H, Sorensen C B, Nygard J and Martinez K L 2012 Cell membrane conformation at vertical nanowire array interface revealed by fluorescence imaging *Nanotechnology* **23** 415102
- [66] Bonde S, Berthing T, Madsen M H, Andersen T K, Buch-Månson N, Guo L, Li X, Badique F, Anselme K, Nygård J and Martinez K L 2013 Tuning InAs Nanowire Density for HEK293 Cell Viability, Adhesion, and Morphology: Perspectives for Nanowire-Based Biosensors *ACS Applied Materials & Interfaces* **5** 10510-9
- [67] Zhao W, Hanson L, Lou H-Y, Akamatsu M, Chowdary P D, Santoro F, Marks J R, Grassart A, Drubin D G, Cui Y and Cui B 2017 Nanoscale manipulation of membrane curvature

- for probing endocytosis in live cells *Nature Nanotechnology* **12** 750
- [68] Dalby M J, Berry C C, Riehle M O, Sutherland D S, Agheli H and Curtis A S 2004 Attempted endocytosis of nano-environment produced by colloidal lithography by human fibroblasts *Experimental cell research* **295** 387-94
- [69] Teo B K K, Goh S-H, Kustandi T S, Loh W W, Low H Y and Yim E K F 2011 The effect of micro and nanotopography on endocytosis in drug and gene delivery systems *Biomaterials* **32** 9866-75
- [70] Galic M, Jeong S, Tsai F C, Joubert L M, Wu Y I, Hahn K M, Cui Y and Meyer T 2012 External push and internal pull forces recruit curvature-sensing N-BAR domain proteins to the plasma membrane *Nature cell biology* **14** 874-81
- [71] Rivnay J, Wang H, Fenno L, Deisseroth K and Malliaras G G 2017 Next-generation probes, particles, and proteins for neural interfacing *Science Advances* **3** e1601649
- [72] Buzsáki G, Anastassiou C A and Koch C 2012 The origin of extracellular fields and currents — EEG, ECoG, LFP and spikes *Nature Reviews Neuroscience* **13** 407-20
- [73] Malkin S L, Kim K K, Tikhonov D B and Zaitsev A V 2014 Properties of spontaneous and miniature excitatory postsynaptic currents in neurons of the rat prefrontal cortex *Journal of Evolutionary Biochemistry and Physiology* **50** 506-14
- [74] Karst H and Joëls M 2005 Corticosterone Slowly Enhances Miniature Excitatory Postsynaptic Current Amplitude in Mice CA1 Hippocampal Cells *Journal of Neurophysiology* **94** 3479-86
- [75] Brette R and Destexhe A 2012 *Handbook of Neural Activity Measurement*, (Cambridge: Cambridge University Press) pp 44-91
- [76] Cao Y, Hjort M, Chen H, Birey F, Leal-Ortiz S A, Han C M, Santiago J G, Pasca S P, Wu J C and Melosh N A 2017 Nondestructive nanostraw intracellular sampling for longitudinal cell monitoring *Proceedings of the National Academy of Sciences of the United States of America* **114** E1866-e74
- [77] VanDersarl J J, Xu A M and Melosh N A 2012 Nanostraws for Direct Fluidic Intracellular Access *Nano Letters* **12** 3881-6
- [78] Xu A M, Wang D S, Shieh P, Cao Y and Melosh N A 2017 Direct Intracellular Delivery of Cell-Impermeable Probes of Protein Glycosylation by Using Nanostraws *ChemBiochem : a European journal of chemical biology* **18** 623-8
- [79] Huang J-A, Caprettini V, Zhao Y, Melle G, Maccaferri N, Deleye L, Zambrana-Puyalto X, Ardini M, Tantussi F, Dipalo M and De Angelis F 2019 On-Demand Intracellular Delivery of Single Particles in Single Cells by 3D Hollow Nanoelectrodes *Nano Letters* **19** 722-31
- [80] Caprettini V, Cerea A, Melle G, Lovato L, Capozza R, Huang J A, Tantussi F, Dipalo M and De Angelis F 2017 Soft electroporation for delivering molecules into tightly adherent mammalian cells through 3D hollow nanoelectrodes *Scientific reports* **7** 8524
- [81] Johansen J P, Diaz-Mataix L, Hamanaka H, Ozawa T, Ycu E, Koivumaa J, Kumar A, Hou M, Deisseroth K, Boyden E S and LeDoux J E 2014 Hebbian and neuromodulatory mechanisms interact to trigger associative memory formation *Proceedings of the National Academy of Sciences* **111** E5584-E92
- [82] Kandel E R 2001 The molecular biology of memory storage: a dialogue between genes and synapses *Science* **294** 1030-8
- [83] Crawford D C and Mennerick S 2012 Presynaptically silent synapses: dormancy and awakening of presynaptic vesicle release *The Neuroscientist : a review journal bringing neurobiology, neurology and psychiatry* **18** 216-23
- [84] Li Y T, Zhang S H, Wang L, Xiao R R, Liu W, Zhang X W, Zhou Z, Amatore C and Huang W H 2014 Nanoelectrode for amperometric monitoring of individual vesicular exocytosis inside single synapses *Angewandte Chemie (International ed. in English)* **53** 12456-60
- [85] Zimmerman J F and Tian B 2018 Nongenetic Optical Methods for Measuring and Modulating Neuronal Response *ACS Nano* **12** 4086-95
- [86] Patolsky F, Timko B P, Yu G, Fang Y, Greytak A B, Zheng G and Lieber C M 2006 Detection, Stimulation, and Inhibition of Neuronal Signals with High-Density Nanowire Transistor Arrays *Science* **313** 1100-4